Agricultural and Forest Meteorology xxx (xxxx) xxx

Contents lists available at ScienceDirect

Agricultural and Forest Meteorology

journal homepage: www.elsevier.com/locate/agrformet

Land-use practices (coppices and dehesas) and management intensity modulate responses of Holm oak growth to drought

Antonio Gazol [a,1,*], Ana-Maria Hereş [b,c,1], Jorge Curiel Yuste [c,d]

[a] Instituto Pirenaico de Ecología (IPE-CSIC), Avenida Montañana 1005, 50059, Zaragoza, Spain
[b] Department of Forest Sciences, Transilvania University of Braşov, Sirul Beethoven -1, 500123 Braşov, Romania
[c] BC3 - Basque Centre for Climate Change, Scientific Campus of the University of the Basque Country, 48940 Leioa, Spain
[d] IKERBASQUE, Basque Foundation for Science, Bilbao, Bizkaia, Spain

ARTICLE INFO

Keywords:
Drought
Holm oak
Land-use practices
Tree rings
Soil
Understorey cover

ABSTRACT

Last decades increase in reported events of drought-induced tree mortality evidences how climate-change is transforming forest ecosystems all over the world. The parallel increase in human pressure over the land is also causing major changes in forest functioning but it remains unclear how these two driving forces interact between them. We combined tree-ring data with aboveground cover, leaf area index (LAI), soil variables, and the standardized precipitation evapotranspiration index (SPEI) as water availability indicator to disentangle the existence of linkages between contrasting Holm oak *(Quercus ilex* L. subsp. *ballota* [Desf.] Samp) land-use practices and its drought-induced decline and mortality. We selected ten sites covering different soil and climatic gradients, land-use practices (i.e., declining dehesas, DH; declining coppices, FRd; and healthy coppices, FRh), and tree vigour classes (i.e., living, affected, and dead trees) in Spain. DH sites presented lower tree coverage, soil water holding capacity and soil pH than coppice (FR) sites. Dead Holm oaks from DH sites were younger than living ones, whereas dead trees from FRd sites were smaller and showed lower growth rates than living ones. We also found that conservation of traditional land-use practices in FR sites, resulting in less understorey cover but more soil erosion (less nutrients and microbial biomass and more bare soil), may positively affect the growth plasticity and sensitivity to drought of Holm oak trees by alleviating inter-specific competition, but in detriment of vegetation cover and soil health. Further studies should evaluate whether what holds true for FRh sites regarding the maintenance of traditional land-use practices might also apply for healthy DH. In the face of drier and hotter scenarios, our results add robust evidences on how the modulation of the intensity of the traditional uses could be a useful tool to optimize ecosystem services in Mediterranean systems highly vulnerable to climate change.

1. Introduction

Temperatures registered in the Mediterranean Basin are already 1.3°C higher than at the beginning of the 20th century which, together with increases in the frequency and severity of drought events (IPCC, 2014), implies serious impacts for natural and semi-natural forest ecosystems (Guiot and Cramer, 2016). Given these conditions and considering that trees' growth under Mediterranean-type climate is strongly limited by water availability (Pasho et al., 2011), it is not surprising that drought-induced tree decline and mortality events have become widespread in such areas within the last decades (Allen et al., 2010; Carnicer et al., 2011; Hereş et al., 2012; Hartmann et al., 2018; Gea-Izquierdo et al., 2019). Even tree species considered to have a marked xylem resistance to drought-induced embolism such as Holm oak (*Quercus ilex* L.) or Cork oak (*Quercus suber* L.) (Gil-Pelegrín et al., 2017) have started to show worrisome signs of decline and mortality in different regions across Spain (Carrasco, 2009; Barbeta et al., 2013; Natalini et al., 2016; Hereş et al., 2018). Consequently, there is an urgent need to advance our understanding on the response of trees to drought and the factors that modulate this response in face of more frequent and severe climate change associated droughts (IPCC, 2014).

Drought-induced decline, usually manifested as foliage loss (Carnicer et al., 2011) and growth reduction (Camarero et al., 2015a,b; Camarero et al., 2018; Hereş et al., 2018), is a consequence of the

* Corresponding author: Antonio Gazol Instituto Pirenaico de Ecología (IPE-CSIC), Avenida Montañana 1005, 50059, Zaragoza, Spain.
E-mail addresses: agazol@ipe.csic.es (A. Gazol), ana_heres@yahoo.com (A.-M. Hereş), jorge.curiel@bc3research.org (J. Curiel Yuste).
[1] have equally contributed to this work

https://doi.org/10.1016/j.agrformet.2020.108235
Received 11 June 2020; Received in revised form 23 September 2020; Accepted 26 October 2020

dysfunction in the hydraulics and carbon allocation of a tree system (Sala et al., 2012). Thus, such relatively short-term external responses of trees to severe drought events (i.e., foliage loss) may be used as possible indicators of internal growth responses (i.e., tree rings) (Hereş et al., 2018). In this sense, annual tree rings provide a retrospective way to quantify growth responses to climate and to evaluate how severe droughts impact tree vigour and modulate the resilience capacity of their growth (Camarero et al., 2015a). The occurrence of consecutive severe drought events may decrease the growth resilience capacity of the trees resulting in negative growth trends (Camarero et al., 2018). Empirical evidence suggests that the secondary growth of Holm oak is sensitive to water scarcity (Gea-Izquierdo et al., 2009). Severe droughts that occurred during the 1990s limited indeed Holm oak growth and impeded its recovery in south-western Spain (Natalini et al., 2016). Also, in north-eastern Spain, the severe droughts that occurred in 2000 and 2005 limited the growth and generated mortality of this species (Galiano et al., 2012; Barbeta et al., 2013). These studies suggest that Holm oak growth decline occurs mainly at warm sites whereas growth enhancement is observed at cold sites (e.g., Gea-Izquierdo et al., 2011) opening thus questions about which factors modulate Holm oak growth responses to drought.

It has been suggested that land-use practices can influence Holm oak growth responses to recent warming trends (e.g., Gea-Izquierdo et al., 2011). Indeed, along with hotter and drier conditions, land-use practices also play a critical role in forest ecosystems' dynamics, as they have the capacity to modulate tree growth-climate relationships (Sangüesa-Barreda et al., 2015; Gentilesca et al., 2017; Jump et al., 2017; Alfaro-Sánchez et al., 2019). Mausolf et al. (2018), for instance, found that the growth response of European beech to extreme climate events differs between ancient and secondary forests. Similarly, the growth response of common temperate oak species to temperature has been found to be contingent on past forest management, with trees from sites with a coppicing history being more sensitive to temperature (Maes et al., 2019).

Holm oak is the most widespread tree species in Spain (Gómez-Aparicio et al., 2011), where its forests have been traditionally subjected for centuries to two major land-use practices: coppices (i.e., forest-like ecosystems) and dehesas (i.e., savannah-like ecosystems; Pulido et al., 2001; Herguido-Sevillano et al., 2017). Holm oak forests that have been coppiced for charcoal and/or firewood production tend to present a multi-stemmed structure and are characterized by a high tree density (Pulido et al., 2001; Herguido-Sevillano et al., 2017). Conversely, the dehesas ecosystems are characterized by a low tree density and are mostly used for livestock rearing and grazing, and for agriculture (Pulido et al., 2001). Land-use practices modify thus the size of the trees and their functional characteristics, making small trees with lower growth rates to be more susceptible to drought-induced decline than large ones as suggested by studies made on different oak species (Galiano et al., 2012; Camarero et al., 2016; Colangelo et al., 2017). However, recent studies suggest that large trees are more prone to drought-induced decline than smaller ones (e.g. Stovall et al. 2019), pointing out the importance of considering this aspect when studying drought-induced forest decline events. During the last decades, the land-use practices gradient has crossed over with another challenge for the Spanish Holm oak coppices and dehesas: the abandonment of these traditional land-use practices (Herguido-Sevillano et al., 2017). This influences how Holm oak trees relate with the understory species (Rolo and Moreno, 2019) and impacts on the plant-soil interactions (Flores-Rentería et al., 2015). Thus, historical land-use practices play a determinant role on how these ecosystems perform (Gentilesca et al., 2017) as they modulate how Holm oak trees grow and respond to climate (Gea-Izquierdo et al., 2011; Martínez-Vilalta et al., 2011). The interaction between drought and land-use practices is therefore of outermost importance to better understand the Holm oak decline and mortality rates registered within the last decades in Spain.

Here we studied Holm oak (*Quercus ilex* L. subsp. *ballota* [Desf.] Samp) growth across different soil and climatic gradients, land-use practices (i.e., declining dehesas, DH; and declining (FRd), and healthy (FRh) coppices), and vigour classes (i.e., living, affected, and dead trees) that currently define Holm oak distribution within the Spanish Iberian Peninsula (hereinafter referred to as Spain to simplify). Our main goal was to disentangle the existence of linkages between Holm oak land-use practices and its drought-induced growth and mortality. For this, we combined tree-ring data with aboveground cover, leaf area index (LAI), soil variables, and the standardized precipitation evapotranspiration index (SPEI) as water availability indicator. Ten Holm oak study sites were carefully selected and used in this study (**Table 1**, **Figure 1**). Our aims were: i) to evaluate whether dead and affected trees differed in age, size, and growth from living ones and, if so, whether these differences were linked with land-use practices (i.e., FR and DH); ii) to disentangle if differences in stand characteristics (aboveground cover, LAI, and soil variables) were linked to land-use practices and/or their abandonment; iii) to evaluate how all this influences Holm oak's growth patterns and responses to drought occurrence in FR and DH.

2. Material and methods

2.1. Studied species and sites

Holm oak (*Quercus ilex* L. subsp. *ballota* [Desf.] Samp) is an evergreen tree species that dominates areas subjected to continental Mediterranean-type climate in the southwestern Europe and North Africa (Rodá et al., 1999). Holm oak growth mainly occurs from April to June and it strongly depends on water availability and mild temperatures at the beginning of the growing season (Campelo et al., 2009; Gea-Izquierdo et al., 2011), while warming trends and severe drought events may constrain its growth during the rest of the growing season (Camarero et al., 2015b; Gentilesca et al., 2017). Holm oak forms a diffuse-to-semi-ring porous wood with multi-seriate rays (Schweingruber, 1990), making tree-ring boundaries to be difficult to be distinguished for this species. Still, several studies performed in recent times have developed reliable tree-ring chronologies on this species (Campelo et al., 2009; Gea-Izquierdo et al., 2011; Natalini et al., 2016; Hereş et al., 2018).

For each of the ten study sites selected for this study (**Table 1**, **Figure 1**), the latitude, longitude, and mean elevation were recorded (**Table 1**). The selection of these study sites was made with the aim of covering: *i)* as uniform as possible different soil (i.e., simplified here to either acidic or basic pH) and climatic gradients (from semi-arid to temperate oceanic; see **Table 1**) where Holm oak may be found; *ii)* representative Holm oak land-use practices (i.e., coppice and dehesas); *iii)* a gradient of Holm oak vigour classes (i.e., quantified here as % of foliar loss or crown defoliation rates) (**Table 1**, **Figure 1**).

Land-use classification was done based on orthophotos, which allowed to precisely estimate the crown coverage (i.e., percentage of trees per ha) of each of our ten study sites (MAGRAMA 2007; Sevilla et al., 2016; García-Angulo et al., 2020), and on in situ observations (i.e., presence or absence of livestock rearing and grazing). The analyses of the orthophotos was done with SigPac viewer (http://signa.ign.es/signa/Pege.aspx) available from the Spanish Ministry of Transport, Mobility and Urban Agenda. Based on this approach, we considered as being dehesas (i.e., DH) the sites where the crown coverage was low (~30% per ha) and where there were clear signs of livestock rearing and grazing. The sites where the crown coverage was high (>30% per ha) and there were not evident signs of livestock rearing and grazing, were considered as being coppices (i.e., FR) (García-Angulo et al., 2020). The ten study sites were further classified based on the vigor class of the Holm oaks by visually estimating the crown defoliation (% of foliage loss) of each Holm oak tree selected (see below). At each site a reference tree was established (i.e., a Holm oak tree with no sign of crown defoliation) and each sampled tree was compared with this reference tree

Table 1
Main characteristics of the ten Holm oak study sites located within Spain. Values in brackets represent standard deviation.

Site (Spanish autonomous community)	Coordinates	Elevation (m a. s.l.)	Land-use practices and tree vigour classes	Climate	Soil pH	Number of trees	DBH (cm)	Age (years)
Huelva (1; Andalucía)	37°59′0.41"N 6°30′43.78"W	418	DH living	Csa	5.53 (acidic)	8	29 (3.31)	111 (17.04)
			DH affected			9	33 (4.48)	97 (15.31)
			DH dead			5	33 (3.13)	83 (12.02)
Talavera de la Reina (2; Castilla-La Mancha)	39°30′6.29"N 4°32′51.21"W	428	DH living	BSk	6.52 (acidic)	4	15 (2.93)	50 (7.93)
			DH affected			4	12 (1.51)	51 (5.00)
			DH dead			6	12 (2.35)	46 (5.04)
Chapinería (3; Madrid)	40°23'3.4"N 4°11'37.8"W	649	DH living	Csa	6.13 (acidic)	9	22 (5.64)	41 (7.79)
			DH affected			9	20 (5.16)	39 (8.22)
			DH dead			9	19 (3.76)	43 (6.59)
Formiche Bajo (4; Aragón)	40°17′49.69"N 0°52′21.32"W	1047	FRd living	Cfb	7.80 (basic)	9	12 (1.95)	56 (5.96)
			FRd affected			7	10 (1.75)	58 (4.28)
			FRd dead			6	8 (0.93)	57 (6.43)
Lleida (5; Cataluña)	41°49′50.60"N 1°27′6.10"E	608	FRd living	BSk	7.51 (basic)	7	20 (2.54)	61 (3.77)
			FRd affected			8	16 (3.43)	59 (12.67)
			FRd dead			8	12 (2.34)	53 (7.01)
Sevilla (6; Andalucía)	37°58′21.91"N 6° 1′10.52"W	727	FRd living	Csa	6.32 (acidic)	9	18 (6.59)	47 (10.50)
			FRd affected			6	13 (5.56)	36 (9.42)
			FRd dead			8	13 (6.14)	43 (17.00)
Almeria (7; Andalucía)	36°53′32.61"N 2°37′4.96"W	944	FRh living	BSk	7.77 (basic)	6	15 (1.47)	61 (18.08)
Arascués (8; Aragón)	42°14′25.43"N 0°26′51.49"W	641	FRh living	Cfb	7.47 (basic)	8	16 (2.30)	67 (11.41)
León (9; Castilla y León)	42°27′0.45"N 5°58′15.48"W	877	FRh living	Cfb	5.30 (acidic)	9	15 (2.12)	35 (13.07)
Navas de Estena (10; Castilla-La Mancha)	39°30′6.29"N 4°32′51.21"W	691	FRh living	BSk	5.55 (acidic)	9	19 (2.01)	64 (6.64)

Where: ***DH living***, living Holm oaks from declining dehesas; ***DH affected***, affected Holm oaks from declining dehesas; ***DH dead***, dead Holm oaks from declining dehesas; ***FRd living***, living Holm oaks from declining coppices; ***FRd affected***, affected Holm oaks from declining coppices; ***FRd dead***, dead Holm oaks from declining coppices; ***FRh living***, living Holm oaks from healthy coppices; ***BSk***, cold semi-arid climate; ***Cfb***, temperate oceanic climate; ***Csa***, hot-summer Mediterranean climate (according to Köppen-Geiger; https://es.climate-data.org/country/5/); ***Number of trees***, the 163 Holm oak trees that were accurately crossdated for the ten study sites; ***DBH (cm)***, mean diameter at breast height for the 163 Holm oak trees that were accurately crossdated for the ten study sites; ***Age (years)***, mean cambial age (i.e., total number of tree rings at standard 1.3 m above ground) of the 151 Holm oak trees included within the analyses. For further details, see the Material and Methods section.

and classified depending on its percentage of foliar loss (i.e., crown defoliation; Dobbertin, 2005) as living (i.e., 0 to 25% crown defoliation), affected (i.e., 25 to 99% crown defoliation), or dead (i.e., 100% crown defoliation). A tree was considered dead if all its stems at the sampling date were completely dry and with no signs of resprouting. Crown defoliation rates were visually evaluated at the whole tree level (i.e., including all its stems when dealing with a multi-stem Holm oak) and were always estimated by the same observer for consistency. Based on the orthophotos, on the in situ observations, and on the individual crown defoliation classifications, we finally had: three declining dehesas (i.e., dehesas where living, affected, and dead Holm oak trees were present; hereinafter referred to as DH), three declining coppices (i.e., coppices where living, affected, and dead Holm oak trees were present; hereinafter referred to as FRd), and four healthy coppices (coppices where only living Holm oak trees were present; hereinafter referred to as FRh) (**Table 1**, **Figure 1**).

2.2. Field sampling and laboratory analyses

2.2.1. Sampling design

We first established three subplots within each of the ten study sites (i.e. 30 in total) to cover as uniform as possible the area of each study site and to account for within site heterogeneity (Garcia-Angulo et al. 2020). To do so, within each study site, we identified three random points (i.e., locations; hereinafter referred to as centroids or central points) around which all needed Holm oaks were sampled (see below). Note that the centroids weren't trees. By using this spatial coverage, we tried to randomize the potential error associated with different micro-environmental conditions that may have also influenced the vigor class of our selected Holm oaks. Our intention was thus to control and minimize the effect of potential confounding factors, finally assuming that the observed variability in crown defoliation (i.e., living, affected, and dead trees) could only be attributed to differences in individual tree physiological responses to drought.

Within each subplot (i.e., around the established centroid) of the three declining dehesas (i.e., DH) we sampled 9 Holm oak trees: 3 living,

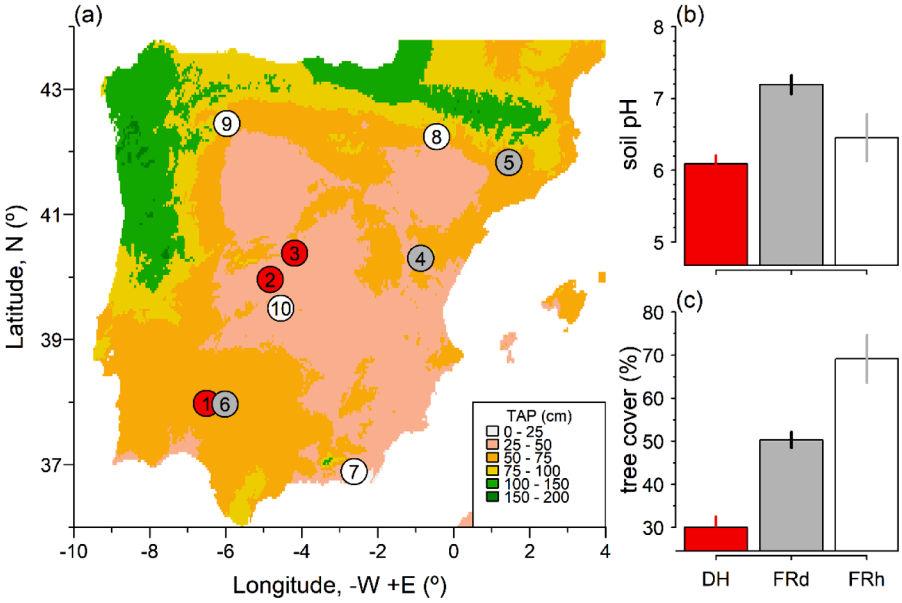

Figure 1. Location of the 10 study sites within Spain, and their characteristics: a) Map indicating the location of the 10 study sites: white dots (healthy coppices, FRh), grey dots (declining coppices, FRd), and red dots (declining dehesas, DH). The background coloured raster of the map represents the total annual precipitation (cm; TAP; according to WorldClim - http s://www.worldclim.org/data/bioclim.html) of Spain); The numbers on the map correspond to the 10 FRh, FRd, and DH study sites mentioned in **Table 1**; b) Averaged soil pH for each land-use practices (i.e., FRh, FRd, and DH); and c) Averaged crown coverage for each land-use practice (i.e., FRh, FRd, and DH).

3 affected, and 3 dead. The same was done for the three declining coppice study sites (i.e., FRd), where we also sampled 3 living, 3 affected, and 3 dead trees in each subplot (i.e., around the established centroid). For the four healthy coppices (i.e., FRh), we only sampled 3 living Holm oaks in each subplot (i.e., around the established centroid) because there were no affected or dead trees at these study sites (cf. *Studied species and sites*). The size of each subplot varied depending on stand density. A total of 198 Holm oaks were selected and sampled for this study. None of the 198 Holm oaks showed evident signs of attack by biotic factors (e.g., insects, fungi). As Holm oaks growing in coppices (i.e., FRd, and FRh) may have a multi-stem structure, when such case was given, we sampled the largest in diameter stem.

2.2.2. *Tree rings*

Field sampling was conducted between October and November 2015 for all study sites except Chapinería that was sampled in October 2010 (see Hereş et al., 2018 for further details on this study site). Tree rings were used to retrospectively study past secondary growth rates (Fritts, 1976) of adult Holm oak trees. To do so, the 198 selected Holm oaks were cored at breast height (i.e., standard 1.3 m above ground) using increment borers of 5 mm diameter (Haglöf, Sweden). Specifically, from each Holm oak, two perpendicular wood cores were extracted and prepared according to standard dendrochronological procedures: air-dried, glued, and polished using a series of sand-paper grids until tree-ring boundaries were clearly visible. The wood cores were then visually crossdated using wide and narrow pointer years (Stokes and Smiley, 1968) and measured to the nearest 0.01 mm using a LINTAB digital positioner and the TSAP-Win^{TM} software (Rinn, 2004). Cross-dating accuracy was repeatedly checked using COFECHA, which calculates moving correlations between each tree-ring series and the mean study site series (Holmes, 1983). In the case of the dead trees, the years of tree mortality were established by attributing calendar years to the outermost tree rings that could be measured. Specifically, this was done using COFECHA, which also runs undated tree-ring series (i.e., individual tree-ring series of dead Holm oaks in this case) against the master chronologies built using the accurately crossdated tree-ring series of the living and affected Holm oaks (Grissino-Mayer, 2001). COFECHA suggested possible dating years for the outermost tree rings of the dead trees, years that were further checked by running the now-dated tree-ring series of the dead trees together with the tree-ring series of the living and affected trees. This process was repeatedly done until all trees have been either accurately crossdated or eliminated from further analyses if not properly crossdated. Note that the confidence of the dating process may have been influenced by the fact that trees might not form tree rings the years immediately before death (Amoroso and Daniels, 2010; Bigler and Rigling, 2013). Accordingly, we here consider the year of mortality to be the outermost tree ring that could be measured. In total, 163 Holm oak trees (**Table 1**) were accurately crossdated for the ten study sites. To highlight the accuracy of our crossdating, we give detailed COFECHA statistics on each of the ten study sites (see **Table S1**). All given COFECHA statistics are in the range of the theoretical values that a ring-width series should have to be considered as correctly cross-dated (see Grissino-Mayer, 2001 for further details).

To remove the trend of decreasing ring width with increasing stem size and tree age over time, and to have a better estimate of the overall tree growth (Biondi and Qeadan, 2008), measured tree-ring widths were transformed into basal area increment (BAI) using the dplR package (Bunn, 2008; Bunn et al., 2020) in the R software (v. 4.0.0, 2020, R Core Team, 2020).

2.2.3. *Aboveground cover and leaf area index*

The aboveground understorey vegetation (surrounding trees, shrubs, and tree seedlings and herbs), stoniness, and bare soil (i.e., non-vegetation) cover were also visually (by consensus among four different observers to maintain the consistency of the data) estimated within a 5 m radius circle around each sampled Holm oak tree as a surrogate for regeneration and competition estimates (Olea and San Miguel, 2006). Specifically, the 5 m radius circle was divided in four equal quadrants, one for each observer. Estimations were done individually by each observer and then averaged among the four observers who agreed on the final, overall estimations. The vegetation cover included herbs (i.e., %), shrubs (i.e., %), and the number of big (i.e., adult trees with a DBH $>$ 15 cm) and small trees (i.e., young trees with a DBH $<$ 15 cm). Stoniness and bare soil were also estimated as percentages. In order to estimate the leaf area index (LAI) of each of our Holm oak trees, three hemispheric photographs were taken at 0.5 m above the ground as centric as possible (i.e., close to the trunk) using a 360° fisheye lens (FCE8, Nikon) and a horizontally-levelled high resolution digital camera (CoolPix 995, Nikon, Tokio, Japan) mounted on a tripod to capture the whole surface of the crowns of the trees. These photographs were further on analyzed with the Hemiview v.2.1 software (Delta-T Devices Ltd, Burwell, UK) and LAI values were calculated for each Holm oak tree.

2.2.4. Soil variables

Soil samples were also collected during the field campaigns, considering the three subplots that were established for each of the ten study sites. Specifically, below each of the selected Holm oak trees, we extracted 3 different soil samples (using a metallic cylinder of 5 cm diameter) to account for the spatial heterogeneity around each of the Holm oaks. The extraction was always done within a radius of 50 cm from the main trunk of the trees and at a depth of 10 cm, after leaf litter removal. Finally, we had 3 composite soil samples for each of the 3 subplots of the ten study sites. Specifically, this was done by mixing per each subplot all the soil samples extracted below the 3 living trees in one bag, all the soil samples extracted below the 3 affected trees in a second bag, and all the soil samples extracted below the 3 dead trees in a third bag. Accordingly, we finally had 9 composite soil samples for each DH and FRd sites, and 3 composite soil samples for each FRh site. This yields a total of 66 soil samples: 54 for the FRd and DH sites, and 12 for the four FRh sites, respectively.

Once collected, soil samples were immediately stored in a portable fridge where a 4 °C temperature was maintained until arrival to the laboratory (García-Angulo et al., 2020). Once in the laboratory, the soil within each bag was homogenized, dried at room temperature, sieved, and used for further analyses. For each soil sample, the pH was measured from a saturated soil paste using a CRISON microp H 2001 (Hach lange Spain, S.L.U., Barcelona, SP), while an elemental analyzer (Thermo Flash 2000, Thermo Fisher Scientific, Waltham, MA, USA) was used to quantify the percentage of total carbon (C) and total nitrogen (N). We also measured the total (P) and available phosphorus (Av P) following the method describe by Burriel and Hernando (1950) and an inductively coupled plasma optical emission spectrometry (PerkinElmer 4300 DV, PerkinElmer Inc., Wellesley, MA, USA). The cation concentration (Ca^{2+}, Mg^{+}, Na^{+}) (M.A.P.A., 1986) was also measured for each soil sample using an inductively coupled plasma optical emission spectrometry (PerkinElmer 4300 DV, PerkinElmer Inc., Wellesley, MA, USA). To determine the amount of ammonium (NH_4^+ - N) the Kjeldahl method (Kjeldahl, 1883) was applied with a continuous flow analyzer (Skalar San++, Skalar Analytical B.V., Breda, The Netherlands). Finally, all these soil variables were expressed per area (m^2) and 10 cm depth using the bulk density which was determined for each soil sample from the volume of the metallic cylinder that we used to extract the soil samples (McKenzie et al., 2004).

Soil heterotrophic CO_2 production (herein after referred to as R_H) was also measured for each of the 66 soil samples using a portable soil gas exchange system (EGM-4, PP systems, MA, USA). This was done using samples of 40 g of dry soil that were placed in glass jars (volume of 150 mL) and rehydrated to their 40% water holding capacity (WHC), following Lucas-Borja et al. (2016). After rewetting, soils were incubated for 48 hours (i.e., at 5, 15, 25, and 35°C) to avoid the Birch effect (Birch, 1958) which consists in potential noises caused by non-linear increases in R_H. Final R_H values are an average of the four R_H values measured at 5, 15, 25, and 35°C as in Garcia-Angulo et al. (2020). R_H was then also calculated per unit of soil organic C content (SOC) as a measurement of soil organic matter (SOM), hereinafter referred to as "C turnover" (Curiel Yuste et al., 2007). Finally, the temperature sensitivity of R_H (Q10) was also calculated and used in further analyses (García-Angulo et al., 2020).

Net N mineralization was also estimated as the change in time of the soil mineral N concentration (i.e., the sum of NO_3^- - N and NH_4^+ - N) (Piccolo et al., 1994). For this, another 40 g of dry soil were placed in glass jars (volume of 150 mL), rehydrated to their 40% water holding capacity (WHC), incubated at 5, 15, 25, and 35°C during 15 days, and measured every 10°C in cycles of 6 hours. Final net N mineralization (i.e., N ammonification, R_{amm}; and N nitrification, R_{nit}) was then calculated as the difference in mineral N between day 15 and day 1 of incubation. Additionally, the nitrification (R_{nit}) was also calculated as the difference in ion nitrate (Piccolo et al. 1994). All these variables have been also expressed per area (m^2) and 10 cm depth following the exact procedure as described before (i.e., mg NH_4^+ - N day^{-1} m^{-2}; mg NO_3^- - N day^{-1} m^{-2}) (García-Angulo et al., 2020).

Soil microbial biomass (i.e., the living soil microbial biomass), was estimated by measuring the maximum respiratory response of each soil sample following Anderson and Domsch (1978). For this, 10 g of dry soil were placed in glass jars (volume of 150 mL) and rehydrated to their 40% water holding capacity (WHC). Then 0.5 g of glucose kg^{-1} of dried soil were added. Finally, these samples were incubated at 30°C for two hours (i.e., the time needed to obtain an initial maximum respiratory response before any increase in microbial biomass). Following the incubation, CO_2 emissions were measured using a portable soil gas exchange system (EGM-4, PP systems, MA, USA). Then, the microbial metabolic quotient (qCO_2) was estimated as the ration between R_H and soil microbial biomass (García-Angulo et al., 2020).

2.2.5. Climatic data

Monthly temperature (T,°C) and precipitation (P, mm) data for each of the ten study sites (**Figure S1**) were downloaded from the Climatic Research Unit (CRU TS3.1; Harris et al., 2014) at a spatial resolution of 0.5 degrees. Monthly climate data was used to calculate the Standardized Precipitation-Evapotranspiration Index (SPEI), which allows for spatial comparability of drought severity, independently of the climatic conditions of each study sites (Vicente-Serrano et al., 2010). SPEI is a multiscalar drought index that may take negative and positive values, indicating dry and wet periods, respectively (Vicente-Serrano et al., 2017; **Figure S1**). We calculated 12-, 18-, and 24-month long June SPEI values for the entire study period (hereinafter referred to as SPEI_JUN12, SPEI_ JUN18, and SPEI_ JUN24) as this scales have been found appropriate for xeric sites (Pasho et al., 2011).

2.2.6. Data analyses

To look for differences between living, affected, and dead trees in coppices and dehesas, we quantified their age, size, and last-decade average growth, growth plasticity, and growth trend. Tree age was estimated by counting the annual tree rings of each Holm oak (i.e., cambial age at standard 1.3 m above ground), and tree size was measured as the diameter at breast height (DBH) (**Table 1**). Note that we were unable to estimate the age of 12 Holm oaks, so the final number of trees included within the analyses was 151. The last-decade average growth was quantified as the average BAI of the last 10 years (hereinafter referred to as BAI10), while the last-decade growth plasticity as the coefficient of variation of BAI for the last 10 years (hereinafter referred to as BAI10cv). Finally, a simple linear regression model was used to estimate the yearly increase or decrease (i.e., trend) in BAI during the last decade (hereinafter referred to as BAI10trend). The 10-year period (i.e., 1999 to 2009) was used to reflect the recent growth characteristics of the trees considering a common period across individuals and sites. We used Linear Mixed-Effects Models (LMEs; Pinheiro et al., 2020) to compare the age, size, and growth features of 151 Holm oaks between land-use practices (i.e., DH, FRd, and FRh). To evaluate whether the land-use practices influenced the sampled Holm oaks, we only compared the living trees from DH, FRd, and FRh sites, as this vigour class was present across the three land-use practices. For each of the variables listed above (i.e. age, size, BAI10, BAI10cv, and BAI10trend), we created a model using land-use practices as fixed factor (DH, FRd, and FRh), and site identity as random factor.

To look for differences between vigour classes within sites, we applied linear regression models. For each of the variables listed above (i.e. age, size, BAI10, BAI10cv, and BAI10trend), we created a model using vigour classes (living, affected, and dead) and site identity as covariates to account for the nested structure of the data. Healthy coppices (i.e., FRh) were removed from this last analysis due to lack of affected and dead trees at these sites. In addition, to account for the potential effect of land-use practices on tree features, we performed the analyses for all sites together but also considering DH and FRd sites separately. When significant differences between vigour classes were

detected, we performed least-square means based on the Tukey HSD honest significant tests (Lenth, 2016).

LMEs were also run to quantify Holm oaks' growth trends and response to drought for the period 1980-2009 as a function of site characteristics (i.e., aboveground cover and soil variables). In this respect, we used Non-Metric Multidimensional Scaling (NMDS; Legendre and Legendre, 2012) with Euclidean dissimilarity to estimate and visualize differences in aboveground vegetation, including understorey vegetation (i.e., herbs, shrubs) as well as adult and young Holm oak trees, stoniness, bare soil cover, and soil variables (hereafter all referred to as NMDS) between sites (**Table S2**). The first axis (NMDS1) clearly separated the DH from FRh and FRd study sites (**Figure 2**), while the second axis (NMDS2) mainly separated FRh from FRd study sites. As expected, NMDS1 was positively correlated with soil bulk density and Av P (available phosphorus) content and negatively with soil pH, total and organic carbon, calcium (Ca^{2+}), and water holding capacity (WHC) and the LAI (leaf area index) of the trees among others (**Table S2**). The NMDS2 was positively correlated with the understorey vegetation cover (shrubs and herbs), and the soil microbial biomass, and negatively with the C/N ratio, LAI and the stoniness and bare soil cover (**Table S2**). PERMANOVA analysis (Permutational Multivariate Analysis of Variance (PERMANOVA; McArdle and Anderson, 2001) confirmed the existence of significant differences between DH, FRh, and FRd ($F = 10.18$; $p < 0.01$; $R^2 = 0.24$). Thus, due to the marked differences between FRh, FRd, and DH sites (**Figure 2**) and the lack of healthy DH sites, separate analyses were performed for DH and FR sites. The second axis of NMDS (i.e., NMDS2) was used to account for differences in aboveground cover (i.e., herbs, shrubs, adult trees, young trees, stoniness, and bare soil) and soil variables between study sites (**Figure 2**). This was done by assigning to each tree the NMDS scores of the subplot to which the tree belonged to.

We restricted the analyses to the 1980-2009 period to avoid the juvenile phase of growth in the youngest trees (see **Table 1** for mean age) and to ensure that all sampled sites span the entire study period. Tree identity was included as random factor to account for the nested structure of the data. Growth trends were quantified by including calendar year as an explanatory variable. Since BAI trajectories can vary along time, we considered linear as well as quadratic potential impacts of calendar year on growth. SPEI_JUN18 was included to account for the response of Holm oak growth to drought. We used the 18 months long SPEI because it had a stronger influence on Holm oak growth than the 12 and 24 months long SPEI's according to LME's (**Table S3**). To account for the differences in growth trajectories and response to drought as a function of NMDS, we included interactions between calendar year, SPEI_JUN18, and NMDS2. Finally, to control for ontogenetic and tree-size factors, age and DBH were included in the fixed part of the models. BAI was log-transformed (log(x+1)) prior to the analyses in order to achieve normality assumptions. We included a first-order autocorrelation structure (AR1) to account for dependency of the BAI in year t (i.e., year of growth) on the BAI of the year t−1 (i.e., previous to growth year). The explanatory variables were standardized by subtracting their means and dividing by their standard deviation to provide comparable coefficients across variables.

To select the most parsimonious models, we applied a multi-model inference approach based on information theory (Burnham and Anderson, 2002). Based on this, we listed the models according to their Akaike Information Criterion (AIC) values. Finally, we selected the most parsimonious model among those models with a difference lower than 2 AIC units from the lowest AIC model. The final selected model was evaluated graphically, and its fit was quantified with a pseudo-R^2 (Nakagawa et al., 2017).

NMDS ordinations and PERMANOVAs were performed applying the "metaMDS" and "adonis" functions from the "vegan" R package (Oksanen et al., 2013). LMEs were carried out with the "nlme" R package (Pinheiro et al., 2020). The "lsmeans" R package (v. 2.30-0) was used to perform least-squares means (Lenth, 2016), while model selection and calculation of model fit were done with the "MuMIn" package (Barton, 2012), and regression plots with the "visreg" (Breheny and Burchett, 2017). All statistical analyses were performed using the R software (v. 4.0.0, 2020, R Core Team, 2020).

3. Results

Holm oak growth (BAI) for the different land-use practices and vigour classes peaked in mid-1990s (~1997) and decreased afterwards (**Figure 3**). In this respect, negative growth trends (i.e., BAI10trend) in the period 1999-2009 were frequent across individuals (**Figure 4**). We found no differences in tree age, size (i.e., DBH), and last-decade growth (i.e., BAI10) and trend (i.e., BAI10trend) between land-use practices (i.e. living trees from DH, FRd, and FRh; **Table S4-S5**). However, we found significant differences in growth plasticity (BAI10cv; **Figure 4**; **Table S5**) with living trees from FRd showing the highest values (0.55 ± 0.02) followed by living trees in DH (0.50 ± 0.03) and living trees in FRh (0.39 ± 0.03). In addition, we found significant differences in age, DBH, and BAI10 between dead, affected, and living trees from DH and FRd sites (**Figure 5**; **Table S6 & Table S9**). Specifically, dead trees were

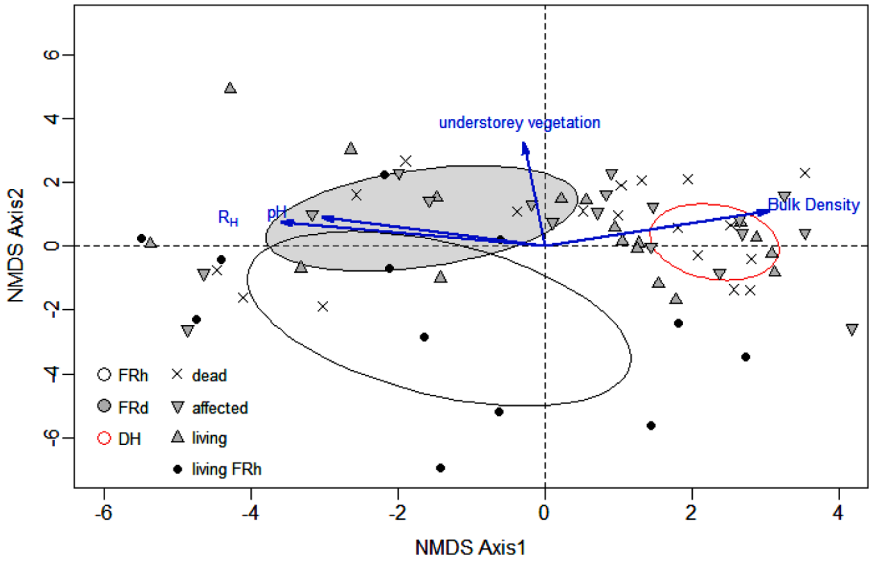

Figure 2. Ordination diagram of Holm oak study sites (66 composite soil samples - 9 for each DH and FRd sites, and 3 for each FRh site) as a function of aboveground cover, LAI, and soil variables (NMDS). The first (NMDS1) and second (NMDS2) axis are shown. Different symbols are used to differentiate between land-use practices and vigour classes: *solid black circles* for living trees from healthy coppice sites (i.e., FRh); *grey triangles up* for living trees from declining coppice and dehesas sites (i.e., FRd, and DH); *grey triangles down* for affected trees from declining coppice and dehesas sites (i.e., FRd, and DH); and *cross symbols* for dead trees from declining coppice and dehesas sites (i.e., FRd, and DH). Ellipsoids represent the hypothetical centroids of the different land-use practices: DH (red area), FRd (grey shaded area), and FRh (black area). Blue arrows represent variables that are strongly correlated with the first or the second NMDS axes (see **Table S2**). *Where*, R_H = soil heterotrophic CO_2 production.

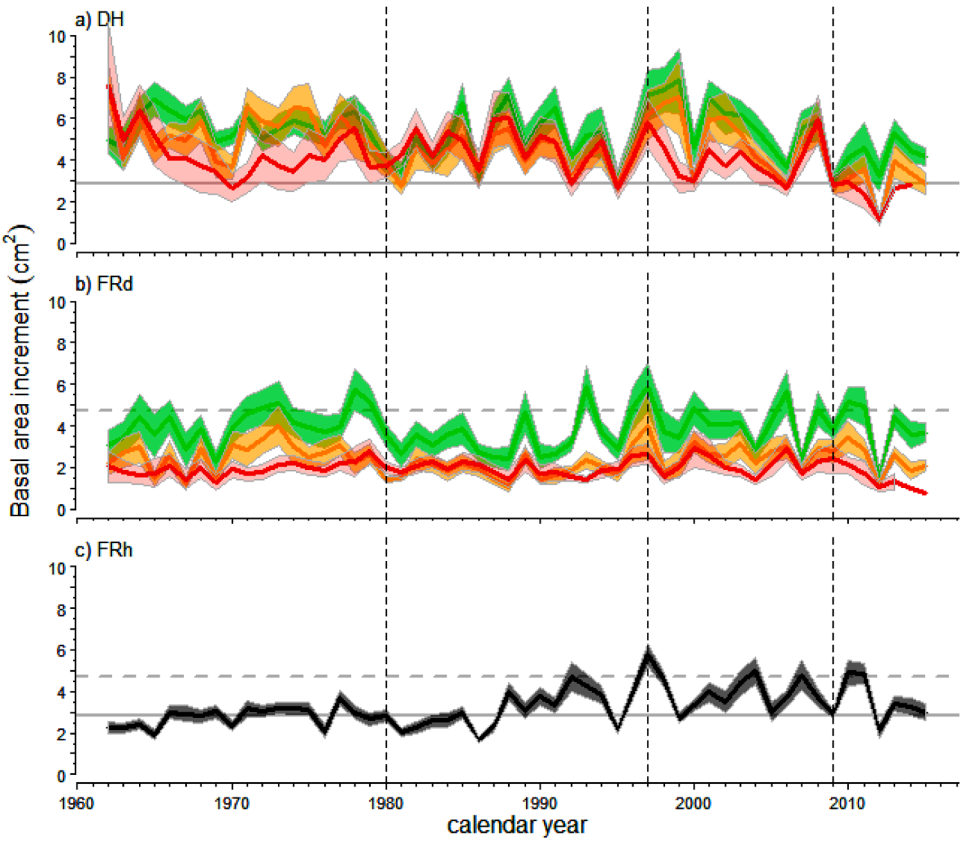

Figure 3. Holm oak growth (BAI) depending on vigour classes: living trees (black) from healthy coppice sites (i.e., FRh), and living (green), affected (orange), and dead (red) trees from declining coppice sites (FRd), and dehesas (DH). Lines represent averages per year across the *n* sites pertaining to each vigour class. Shaded areas of each vigour class represent standard errors of the mean. The grey solid lines represent mean BAI values of the FRd sites within the DH and FRh graphs, whereas dashed lines represent mean BAI values of DH within the FRd and FRh graphs. Vertical dashed lines indicate the 1980, 1999, and 2009 years that were used to delimitate different study periods (cf. *Data analyses*).

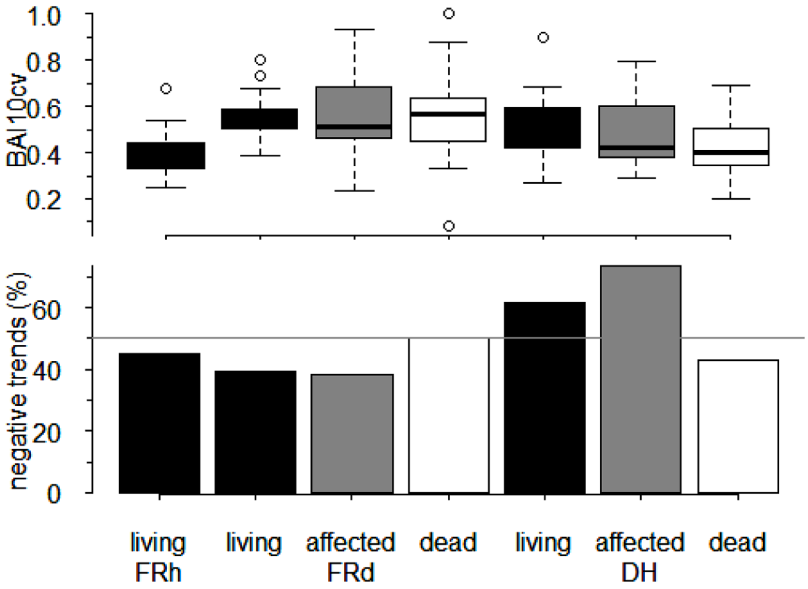

Figure 4. Differences in tree features between vigour classes (i.e., living, affected, and dead Holm oaks) and land-use practices (i.e. dehesas (i.e., DH), and coppice sites (FRd, and FRh)). *Where*, BAI10cv = last-decade growth plasticity; negative trends (%) = the percentage of trees that displayed negative growth trends for the last 10 years (i.e. negative BAI10trend values). Last 10 years refers to the period from 1999 to 2009.

younger and showed lower DBH and BAI10 than coexisting living trees. Furthermore, affected trees, presented lower BAI10 than coexisting living ones (Figure 5; **Table S9**). When DH and FRd were analysed separately (Figure 5; **Table S7-S9**), we found that living trees were significantly older than coexisting dead individuals in DH (Figure 5; **Table S9**), whereas no age differences were found between living, affected, and dead trees in FRd sites (Figure 5). Instead, living trees from the FRd study sites presented significantly larger DBH and BAI10 than coexisting affected and dead trees (Figure 5; **Table S9**).

Linear Mixed-Effects Models, performed with BAI for the 1980-2009 period, pointed out the existence of significant differences in growth trends (only for FR sites) and responses to drought intensity as a function of NMDS (i.e., LAI, understorey vegetation cover and soil variables) (Table 2; Figure 6-7). For the DH sites, the final selected model (i.e. the

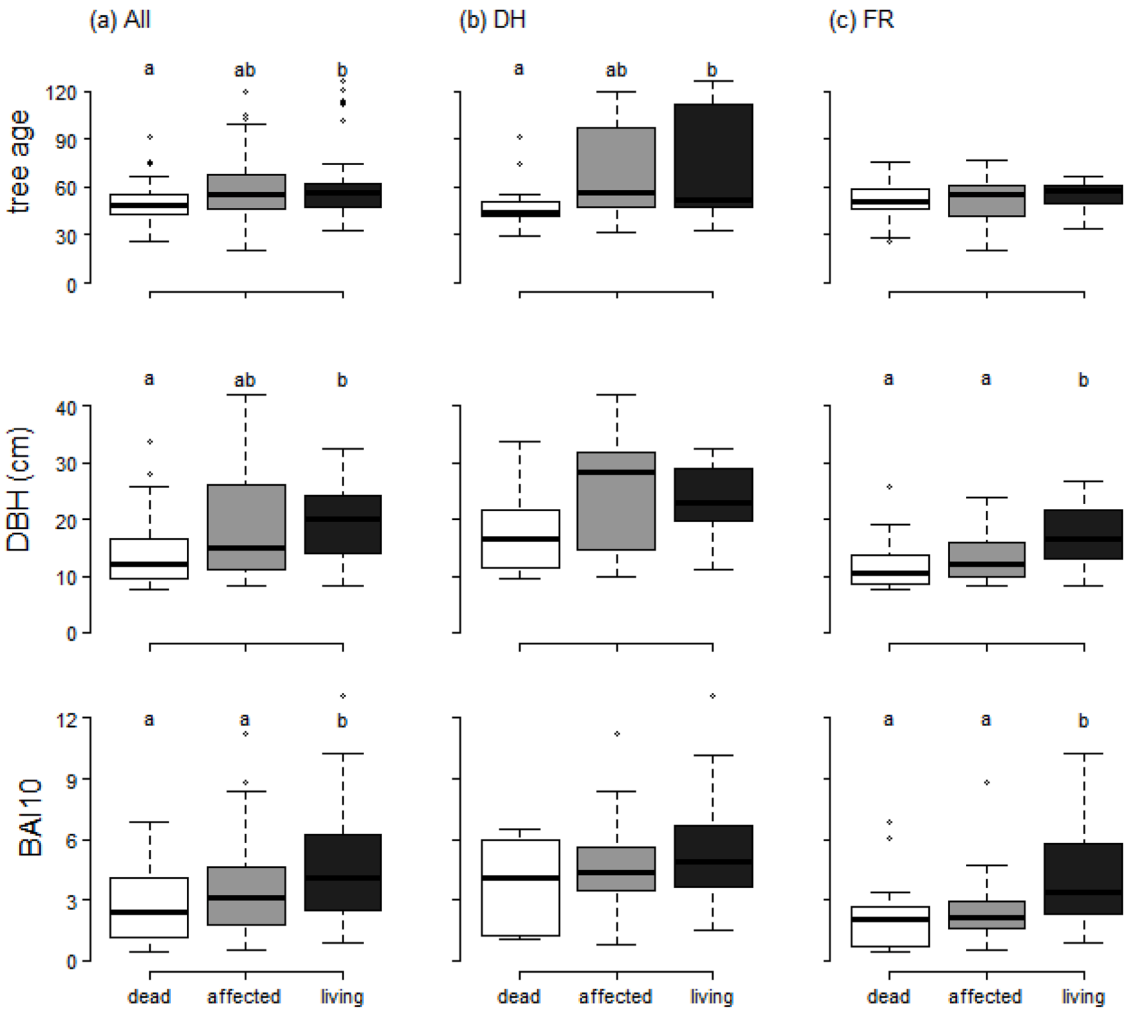

Figure 5. Differences in tree features between vigour classes (i.e., living, affected, and dead Holm oaks) considering a) both declining dehesas (i.e., DH) and coppice sites (FRd); declining dehesas (i.e., DH) only; and c) coppice sites (FRd)only. *Where*, tree age = estimated cambial age; DBH (cm) = diameter at breast height; BAI10 = last-decade average growth. Different letters indicate the existence of significant ($p < 0.05$) differences between vigour classes (see **Table S9**).

most parsimonious model between those models with ΔAIC <= 2) accounted for 55% of the variation in the data (44% due to the fixed factors alone). The model included tree age, DBH, NMDS2, linear and quadratic functions of calendar year, SPEI_JUN18, and interactions between SPEI_JUN18 and NMDS2 (**Table 2; Table S10**). For the FR sites, the final model accounted for 51% of the variation in BAI (49% due to the fixed factors alone) and included the same factors as for the DH sites, but also interactions between them (**Table 2; Table S10**). For both DH and FR sites, Holm oak's growth decreased with tree age and NMDS2, and increased with DBH and the increase in SPEI_JUN18 (Table 2). The interaction between calendar year (quadratic term) and NMDS2 showed that FR trees that corresponded to negative NMDS2 scores (less understorey cover but more eroded soils, i.e. more stoniness and bare soil, less microbial biomass) presented a unimodal BAI over the 1980-2009 period, with a growth peak in the middle of the period. Conversely, trees that corresponded to positive NMDS2 scores (high understorey cover and soils less eroded) presented a more linear growth trend (Figure 6). The interaction between SPEI_JUN18 and NMDS2 indicated a greater responsiveness to SPEI_JUN18 of DH and FR trees with low scores in NMDS2 (Figure 7).

4. Discussion

We combined tree-ring data with aboveground cover, leaf area index (LAI), soil variables, and the standardized precipitation evapotranspiration index (SPEI) as water availability indicator to disentangle the existence of linkages between Holm oak land-use practices and its drought-induced decline and mortality. Dehesas (DH) and coppice (FR) study sites proved to be clearly different when soil variables and LAI were analysed, which might have in turn underlined the differences between living, affected, and dead Holm oaks. Our results clearly show how both, potential causes of tree mortality as well as historical growth trends, differed markedly between stands that have been subjected to those two traditional land-use practices. We, therefore, collected compelling evidences on how anthropic interventions over these systems, through the conservation of traditional uses and/or the modulation of the management intensity, may serve as a potential efficient tool to adapt Holm oak systems to a drier and hotter future where human pressure over land is also increasing.

4.1. Effects of land-use practices on tree health

We found that dead Holm oak trees were younger than the living Holm oak trees in DH, while dead Holm oak trees presented lower growth rates than the living Holm oak trees in the declining coppices (FRd) (Figure 5; **Table S9**). Our results, therefore, bring novelty as they clearly suggest that different processes govern Holm oak health, including its decline and mortality, under different land-use practices (i.e., DH and FRd). Holm oak mortality in FRd have been generally explained by density depended and linked to competition for water

Table 2
Results of Linear Mixed-Effects Models (LMEs) built to quantify Holm oaks' growth trends and response to drought intensity for the period 1980-2009 as a function NMDS (i.e., aboveground cover and soil variables). The variables included in the selected model are shown together with their associated standardized coefficients (± Standard Error), t-statistic, and p-values (* for $p < 0.05$, ** for $p < 0.01$, *** for $p < 0.001$).

Variables	DH standardized (± SE)	t-value	FRd and FRh standardized (± SE)	t-value
Age	-0.17 ± 0.02	-8.52**	-0.06 ± 0.006	-9.94**
DBH	0.26 ± 0.02	12.08**	0.18 ± 0.007	27.77**
NMDS2	-0.01 ± 0.01	-1.02	-0.05 ± 0.008	-6.84**
Year (linear term)	0.005 ± 0.005	0.90	0.03 ± 0.004	7.11**
Year (quadratic term)	-0.02 ± 0.006	-4.17**	-0.006 ± 0.005	-1.37
SPEI_JUN18	0.04 ± 0.004	9.05**	0.02 ± 0.003	5.50**
Year (linear term) * NMDS2	-		-0.003 ± 0.004	-0.70
Year (quadratic term) * NMDS2	-		0.02 ± 0.005	4.33**
SPEI_JUN18 * NMDS2	0.01 ± 0.004	3.39**	-0.02 ± 0.003	-4.84**

Where, DH = declining dehesas, FRd = declining coppice sites; FRh = healthy coppice sites; DBH = diameter at breast height; NMDS2 = second axis of NMDS; Year (linear term) = linear potential impacts of calendar year on growth; Year (quadratic term) = quadratic potential impacts of calendar year on growth; SPEI_JUN18 = 18 months long SPEI (Standardized Precipitation-Evapotranspiration Index); (cf. *Data analyses* for further details on the variables).

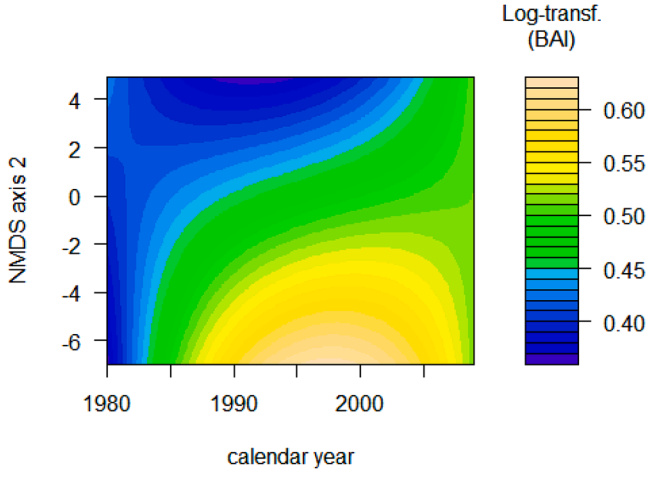

Figure 6. Contour plot representing the interaction between calendar year and the second axis of NMDS (i.e., NMDS2) according to the Linear Mixed-Effects Models (LMEs) results for the coppice sites (i.e., FRd and FRh; see **Table 2**). Colours represent log-transformed BAI values from low (blue) to high (salmon).

resources (Gómez-Aparicio et al., 2011; Galiano et al., 2012). Along this, recent studies performed on oak species suggest that small trees with lower growth rates can be more vulnerable to drought (Colangelo et al., 2017; Gentilesca et al., 2017). This contrasts with the also found greater drought-sensitivity of larger trees (Stovall et al., 2019), but can be partially explained by the multi-stem structure of Holm oaks in coppice stands (Galiano et al 2012). Thus, our results reinforce the results of these studies indicating that in dense stands small Holm oaks with lower growth rates might be more susceptible to succumb to death because of severe droughts.

In ecosystems where water is not necessarily the limiting factor because the tree density cover is low and the shrubs are scarce, other processes emerged as potential causes of tree vulnerability. The fact that the dead trees from DH were younger than the living trees, althought of similar size, suggests that those trees growing faster were the most

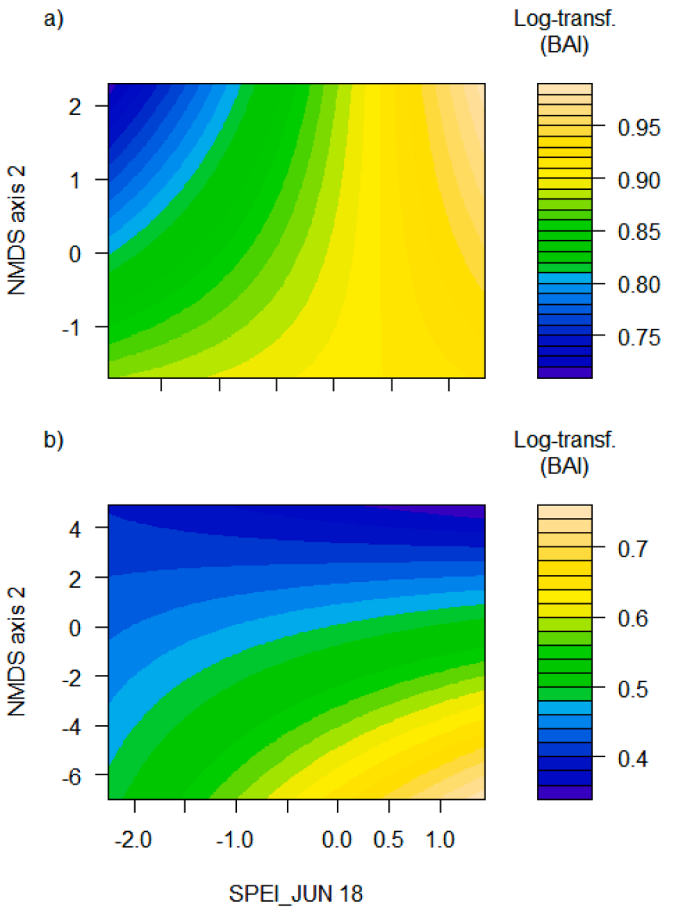

Figure 7. Contour plot representing the interaction between the SPEI_JUN18 and the second axis of NMDS (i.e., NMDS2) according to the Linear Mixed-Effects Models (LMEs) results for the a) dehesas (i.e. DH); and b) coppice sites (i.e., FRd and FRh; see **Table 2**). Colours represent log-transformed BAI values from low (blue) to high (salmon).

vulnerable to drought (i.e. growth-lifespan trade-offs; Büntgen et al. 2019, Brienen et al. 2020). Another potential interpretation of these results could be that the abandonment of traditional land-use practices, occurred during the last decades, may have determined the establishment of young trees in less favourable environments making them more vulnerable to different threats (Herguido-Sevillano et al., 2017). However, further studies are required to disentangle whether the higher vulnerability of younger trees to die is influenced by land abandonment, microsite conditions, or purely physiological trade-offs between tree growth and their longevity. The comparison of the growth of Holm oaks in healthy and declining dehesas may help obtain more robust conclusions in this regard.

4.2. *Effects of land-use practices on tree growth historical trends*

We also found that differences in tree growth could be linked to land-use practices and management intensity, as we found a link between the understorey cover, soil erosion, and Holm oak growth plasticity and capacity to respond to drought. This relationship was more intense in FR sites and suggests that differences in Holm oak secondary growth trends between declining and healthy coppice stands (i.e. FRd and FRh) may depend on the maintenance of traditional land-use practices (**Table 2**; **Figures 6-7**). The lack of management in FRd may promote successional vegetation growth (including shrubs, seedlings, and herbs) thus increasing the competition between Holm oak and the understorey (Rolo and Moreno, 2019). However, higher understorey vegetation cover can be also a secondary effect of tree mortality, which allowed

higher light availability at the floor level and decreased competition for water. In the past, thinning was used to reduce stand density and thus the tree to tree competition for water and other resources was also alleviated (Gómez-Aparicio et al., 2011; Gentilesca et al., 2017). It has been suggested that shrub encroachment, because of the abandonment of traditional land-uses in Holm oak ecosystems, may exacerbate the consequences of drought on Holm oak productivity (Rolo and Moreno, 2019). Thus, it is plausible to think that greater inter-specific competition, either with other trees or large shrubs and herbs, can lead to Holm oak decline (Martínez-Vilalta et al., 2011). Our results point in this direction indicating that Holm oak growth trends and responses to drought intensity were modulated by the alignment of sites across gradients of understorey vegetation cover and soil degradation that are determined by the land-use intensity. Indeed, land abandonment may result in the recovery of soil health but also in denser understories that may favour oak recruitment (Gómez-Aparicio et al., 2005) but that can reverse into competition with the overstorey as the understory becomes denser and more dominant.

Vertical partition of soil resources between Holm oak and the accompanying aboveground vegetation cover may reduce competition intensity (Barbeta et al., 2013; Barbeta et al., 2017). Accordingly, while herbaceous species will have a dense network of roots in the first topsoil centimetres, oaks will explore deeper niches (Barbeta et al., 2017). However, shrubs and small trees from the aboveground vegetation cover could also reach the same deep soil layers as Holm oak, enhancing thus the competition for water and other resources (Rolo and Moreno, 2019). In this sense, observed differences in key functional traits of the microbial communities (more biomass in declining sites with respect to healthy ones) could have suggested that competition for nutrients among larger microbial communities, able to retain more nutrients and compete more efficiently for resources, could partially explain the lack of tree responsiveness in sites with more aboveground vegetation cover (Jacoby et al., 2017). However, no differences in oligonutrient availability and increased values of N were associated with decline (**Table S2**) suggesting that in this semiarid region competition between trees and the aboveground vegetation cover may be especially focused in obtaining water.

In summary, our results concur with previous findings that land-use practices modulate forest growth (Sangüesa-Barreda et al., 2015; Gentilesca et al., 2017; Mausolf et al., 2018; Alfaro-Sánchez et al. 2019; Maes et al., 2019). This pattern was more evident in coppices than in dehesas (**Figure 7**; **Table 2**), probably because of the larger NMDS2 gradient in the coppices. The selection of the ten study sites considered for this study has been carefully done trying to cover as uniform as possible different soil and climatic gradients, land-use practices, and vigour classes that currently define Holm oak distribution within Spain. Nevertheless, this uniformity has been determined and affected by uncontrollable factors such as the lack of healthy DH among the studied sites due to logistic. Healthy DH would have allowed us more robust statistical conclusions and a more in depth understanding of the role of traditional practices associated with this particular land-use (e.g. livestock load, ploughing for cultivation between trees, tree pruning) on the growth and health of Holm oaks. For instance, it is well known that the lack of tree recruitment due to livestock browse, or the increased occurrence of soil-borne pathogens like *Phytophthora cinnamomi* (Corcobado et al., 2013; de Sampaio et al., 2013), whose propagation in soil is enhanced by ploughing, are well known to threaten the health of Holm oak trees in DH. Thus, further studies are required to understand the role of traditional practices on the conservation of Holm oak health in dehesas.

5. Conclusions

The linkages between site conditions and growth patterns observed in this study suggest that the intensity and the land-use practices at which Holm oak stands are subjected partially determine Holm oak performance in drier scenarios. Relaxing competition for resources by maintaining historical practices, even in detriment of soil quality, improves Holm oak growth. However, relaxing the intensity of the practices resulted in an increase in vegetation cover (due to a secondary successional process) and in soil health (increase in microbial biomass, soil N concentration and C turnover) that may revert in an improvement in the capacity of this systems to provide other important services of, e.g. mitigation, such as C sequestration, in detriment of the health of the Holm oaks. In the face of drier and hotter scenarios, our results reveal how modulation of the intensity of the traditional land-uses can be a useful tool to optimize the ecosystem services of these Mediterranean systems highly vulnerable to climate change (Astigarraga et al. 2020).

Declaration of Competing Interest

The authors declare that they have no known competing financial interests or personal relationships that could have appeared to influence the work reported in this paper.

Acknowledgements

This research was funded by the Spanish Government projects VERONICA (CGL2013-527 42271-P) and IBERYCA (CGL2017-84723-P). Additionally, it was also supported by the Basque Government through the BERC 2018-2021 program, and by the Spanish Ministry of Science, Innovation and Universities through the BC3 María de Maeztu excellence accreditation (MDM-2017-0714). Ana-Maria Hereş was financially supported by the projects NATIvE (PN-III-P1-1.1-PD-2016-0583) and REASONING (PN-III-P1-1.1-TE-2019-1099), both funded by the Romanian Ministry of National Education and by the Romanian Ministry of Research and Innovation through UEFISCDI (link). A. Gazol acknowledges funding by project RTI2018-096884-B-C31 (Spanish Ministry of Science). We thank Daniel García Angulo, Miguel Fernandez, David López Quiroga, Bárbara Carvalho, Matheus Lopes Souza, and Mario Díaz for their priceless support during the field campaigns and the laboratory work.

Supplementary materials

Supplementary material associated with this article can be found, in the online version, at doi:10.1016/j.agrformet.2020.108235.

BIBLIOGRAPHY

Alfaro-Sánchez, R., Jump, A.S., Pino, J., Díez-Nogales, O., Espelta, J.M., 2019. Land use legacies drive higher growth, lower wood density and enhanced climatic sensitivity in recently established forests. Agricultural and Forest Meteorology 276–277, 107630.

Allen, C.D., Macalady, A.K., Chenchouni, H., Bachelet, D., McDowell, N., Vennetier, M., Kitzberger, T., Rigling, A., Breshears, D.D., Hogg, E.H., Gonzalez, P., Fensham, R., Zhang, Z., Castro, J., Demidova, N., Lim, J.H., Allard, G., Running, S.W., Semerci, A., Cobb, N., 2010. A global overview of drought and heat-induced tree mortality reveals emerging climate change risks for forests. Forest Ecology and Management 259, 660–684.

Amoroso, M.M., Daniels, L.D., 2010. Cambial mortality in declining *Austrocedrus chilensis* forests: implication for stand dynamics studies. Canadian Journal of Forest Research 40, 885–893.

Anderson, J.P.E., Domsch, K.H., 1978. A physiological method for the quantitative measurement of microbial biomass in soils. Soil Biology & Biochemistry 10, 215–221.

Astigarraga, J., Andivia, E., Zavala, M.A., Gazol, A., Cruz-Alonso, V., Vicente-Serrano, S. M., Ruiz-Benito, P., 2020. Evidence of non-stationary relationships between climate and forest responses: increased sensitivity to climate change in Iberian forests. Global Change Biology. https://doi.org/10.1111/gcb.15198. Accepted Author Manuscript.

Barbeta, A., Ogaya, R., Peñuelas, J., 2013. Dampening effects of long-term experimental drought on growth and mortality rates of a holm oak forest. Global Change Biology 19, 3133–3144.

Barbeta, A., Peñuelas, J., 2017. Increasing carbon discrimination rates and depth of water uptake favor the growth of Mediterranean evergreen trees in the ecotone with temperate deciduous forests. Global Change Biology 23, 5054–5068.

Barton, K., 2012. MuMIn: Multi-model inference. (R package version 1.7.7) 2012 Available at http://CRAN.R-project.org/package=MuMIn .
Bigler, C., Rigling, A., 2013. Precision and accuracy of tree-ring-based death dates of mountain pines in the Swiss National Park. Trees 27, 1703–1712.
Biondi, F., Qeadan, F., 2008. A theory-driven approach to tree-ring standardization: defining the biological trend from expected basal area increment. Tree-Ring Research 64, 81–96.
Birch, H.F., 1958. The effect of soil drying on humus decomposition and nitrogen availability. Plant and Soil 10, 9–31.
Breheny, P, Burchett, W, 2017. Visualization of Regression Models Using visreg. The R Journal 9, 56–71. https://doi.org/10.32614/RJ-2017-046.
Brienen, R.J.W., Caldwell, L., Duchesne, L., Voelker, S., Barichivich, J., Baliva, M., Ceccantini, G., Di Filippo, A., Helama, S., Locosselli, G.M., Lopez, L., Piovesan, G., Schöngart, J., Villalba, R., Gloor, E., 2020. Forest carbon sink neutralized by pervasive growth-lifespan trade-offs. Nature Communications 11, 4241. https://doi.org/10.1038/s41467-020-17966-z.
Bunn, A.G., 2008. A dendrochronology program library in R (dplR). Dendrochronologia 26, 115–124.
Bunn, A.G., Korpela, M., Biondi, F., Campelo, F., Mérian, P., Qeadan, F., Zang, C., 2020. dplR: Dendrochronology Program Library in R. R package version 1.7.1. https://CRAN.R-project.org/package=dplR.
Burnham, K.P., Anderson, D.R., 2002. Model selection and multimodel inference. A practical information – theoretic approach, Second edition. Springer-Verlag Press, New York.
Burriel, F., Hernando, V., 1950. El fósforo en los suelos españoles. V. Nuevo método para la determinar el fósforo asimilable en los suelos. Anales de Edafología y Agrobiologia 9, 611–622.
Büntgen, U., Krusic, P.J., Piermattei, A., Coomes, D.A., Esper, J., Myglan, V.S., Kirdyanov, A.V., Camarero, J.J., Crivellaro, A., Körner, C., 2019. Limited capacity of tree growth to mitigate the global greenhouse effect under predicted warming. Nature Communications 10, 2171.
Carrasco, A., 2009. Procesos de Decaimiento Forestal (La Seca): Situación del Conocimiento. Consejería de Medio Ambiente, 98 pp. Juntade Andalucía, Córdoba, Spain.
Camarero, J.J., Gazol, A., Sangüesa-Barreda, G., Oliva, J., Vicente-Serrano, S.M., 2015a. To die or not to die: early warnings of tree dieback in response to a severe drought. Journal of Ecology 103, 44–57.
Camarero, J.J., Franquesa, M., Sangüesa-Barreda, G., 2015b. Timing of drought triggers distinct growth responses in holm oak: implications to predict warming-induced forest defoliation and growth decline. Forests 6, 1576–1597.
Camarero, J.J., Sangüesa-Barreda, G., Vergarechea, M., 2016. Prior height, growth, and wood anatomy differently predispose to drought-induced dieback in two Mediterranean oak species. Annals of Forest Science 73, 341–351.
Camarero, J.J., Gazol, A., Sangüesa-Barreda, G., Cantero, A., Sánchez-Salguero, R., Sánchez-Miranda, A., Granda, E., Serra-Maluquer, X., Ibañez, R., 2018. Forest growth responses to drought at short- and long-term scales in Spain: squeezing the stress memory from tree rings. Frontiers in Ecology and Evolution 6 (9).
Campelo, F., Nabais, C., García-González, I., Cherubini, P., Gutiérrez, E., Freitas, H., 2009. Dendrochronology of Quercus ilex L. and its potential use for climate reconstruction in the Mediterranean region. Canadian Journal of Forest Research 39, 2486–2493.
Carnicer, J., Coll, M., Ninyerola, M., Pons, X., Sánchez, G., Peñuelas, J., 2011. Widespread crown condition decline, food web disruption, and amplified tree mortality with increased climate change-type drought. Proceedings of the National Academy of Sciences of the United States of America 108, 1474–1478.
Colangelo, M., Camarero, J.J., Borghetti, M., Gazol, A., Gentilesca, T., Ripullone, F., 2017. Size matters a lot: drought-affected Italian oaks are smaller and show lower growth prior to tree death. Frontiers in Plant Science 8, 135.
Corcobado, T., Cubera, E., Moreno, G., Solla, A., 2013. Quercus ilex forests are influenced by annual variations in water table, soil water deficit and fine root loss caused by Phytophthora cinnamomi. Agricultural and Forest Meteorology 169, 92–99.
Curiel Yuste, J., Baldocchi, D.D., Gershenson, A., Goldstein, A, Misson, L., Wong, S., 2007. Microbial soil respiration and its dependency on carbon inputs, soil temperature and moisture. Global Change Biology 13, 2018–2035.
de Sampaio e Paiva Camilo-Alves, C., da Clara, M.I.E., de Almeida Ribeiro, N.M.C., 2013. Decline of Mediterranean oak trees and its association with Phytophthora cinnamomi: a review. European Journal Forest Research, 132, 411–432.
Dobbertin, M., 2005. Tree growth as indicator of tree vitality and of tree reaction to environmental stress: a review. European Journal Forest Research 124, 319–333.
Flores-Rentería, D., Curiel Yuste, J., Rincón, A., Brearley, F., García-Gil, J., Valladares, F., 2015. Habitat fragmentation can modulate drought effects on the plant-soil-microbial system in Mediterranean holm oak (*Quercus ilex*) forests. Microbial Ecology 69, 798e812.
Fritts, H.C., 1976. Tree Rings and Climate. Academic Press, London, United Kingdom.
Galiano, L., Martínez-Vilalta, J., Sabaté, S., Lloret, F., 2012. Determinants of drought effects on crown condition and their relationship with depletion of carbon reserves in a Mediterranean holm oak forest. Tree Physiology 32, 478–489.
García-Angulo, D., Hereş, A.-M., Fernández-López, M., Flores, O., Sanz, M.J., Rey, A., Valladares, F., Curie Yuste, J., 2020. Holm oak decline and mortality exacerbates drought effects on soil biogeochemical cycling and soil microbial communities across a climatic gradient. Soil Biology & Biochemistry 149. https://doi.org/10.1016/j.soilbio.2020.107921.
Gea-Izquierdo, G., Martín-Benito, D., Cherubini, P., Cañellas, I., 2009. Climate-growth variability in Quercus ilex L. west Iberian open woodlands of different stand density. Annals of Forest Science 66, 802. https://doi.org/10.1051/forest/2009080.
Gea-Izquierdo, G., Cherubini, P., Cañellas, I., 2011. Tree-rings reflect the impact of climate change on Quercus ilex L. along a temperature gradient in Spain over the last 100 years. Forest Ecology and Management 262, 1807–1816.
Gea-Izquierdo, G., Férriz, M., García-Garrido, S., Aguín, O., Elvira-Recuenco, M., Hernández-Escribano, L., Martín-Benito, D., Raposo, R., 2019. Synergistic abiotic and biotic stressors explain widespread decline of Pinus pinaster in a mixed forest. Science of the Total Environment 685, 963–975.
Gentilesca, T., Camarero, J.J., Colangelo, M., Nolè, A., Ripullone, F., 2017. Drought-induced oak decline in the western Mediterranean region: an overview on current evidences, mechanisms and management options to improve forest resilience. iForest 10, 796–806.
Gil-Pelegrín, E., Peguero-Pina, J.J., Sancho-Knapik, D., 2017. Oaks physiological ecology. Exploring the functional diversity of genus Quercus L. Springer International Publishing, AG, Switzerland.
Gómez-Aparicio, L., Gómez, J.M., Zamora, R., Boettinger, J.L., 2005. Canopy vs. soil effects of shrubs facilitating tree seedlings in Mediterranean montane ecosystems. Journal of Vegetation Science 16, 191–198.
Gómez-Aparicio, L., García-Valdés, R., Ruiz-Benito, P., Zavala, M.A., 2011. Disentangling the relative importance of climate, size and competition on tree growth in Iberian forests: implications for forest management under global change. Global Change Biology 17, 2400–2414.
Grissino-Mayer, H.D., 2001. Evaluating crossdating accuracy: a manual and tutorial for the computer program COFECHA. Tree-Ring Research 57, 205–221.
Guiot, J., Cramer, W., 2016. Climate change: the 2015 Paris Agreement thresholds and Mediterranean basin ecosystems. Science 354, 465–468.
Harris, I., Jones, P.D., Osborn, T.J., Lister, D.H., 2014. Updated high-resolution grids of monthly climatic observations – the CRU TS3.10 Dataset. International Journal of Climatology 34, 623–642.
Hartmann, H., Moura, C.F., Anderegg, W.R.L., Ruehr, N.K., Salmon, Y., Allen, C.D., 2018. Research frontiers for improving our understanding of drought-induced tree and forest mortality. New Phytologyst 218, 15–28.
Herguido-Sevillano, E., Lavado Contador, J.F., Pulido, M., Schnabel, S., 2017. Spatial patterns of lost and remaining trees in the Iberian wooded rangelands. Applied Geography 87, 170–183.
Hereş, A.M., Martínez-Vilalta, J., Claramunt López, B., 2012. Growth patterns in relation to drought-induced mortality at two Scots pine (Pinus sylvestris L.) sites in NE Iberian Peninsula. Trees 26, 621–630.
Hereş, A.M., Kaye, M.W., Granda, E., Benavides, R., Lázaro-Nogal, A., Rubio-Casal, A.E., Valladares, F., Curiel Yuste, J., 2018. Tree vigour influences secondary growth but not responsiveness to climatic variability in Holm oak. Dendrochronologia 49, 68–76.
Holmes, R.L., 1983. Computer-assisted quality control in tree-ring dating and measurement. Tree-Ring Bulletin 43, 69–78.
IPCC, 2014. Climate change 2014: impacts, adaptation, and vulnerability. In: Field, C.B., Barros, V.R., Dokken, D.J., Mach, K.J., Mastrandrea, M.D., Bilir, T.E., Chatterjee, M., Ebi, K.L., Estrada, Y.O., Genova, R.C., Girma, B., Kissel, E.S., Levy, A.N., MacCracken, S., Mastrandrea, P.R., White, L.L. (Eds.), Part A: Global and Sectoral Aspects. Contribution of Working Group II to the Fifth Assessment Report of the Intergovernmental Panel on Climate Change. Cambridge University Press, Cambridge, United Kingdom and New York, NY, USA.
Jacoby, R., Peukert, M., Succurro, A., Koprivova, A., Kopriva, S., 2017. The Role of Soil Microorganisms in Plant Mineral Nutrition —Current Knowledge and Future Directions. Frontiers in Plant Science 8, 1617.
Jump, A.S., Ruiz-Benito, P., Greenwood, S., Allen, C.D., Kitzberger, T., Fensham, R., Martínez-Vilalta, J., Lloret, F., 2017. Structural overshoot of tree growth with climate variability and the global spectrum of drought-induced forest dieback. Global Change Biology 23, 3742–3757.
Kjeldahl, J., 1883. Neue Methode zur Bestimmung 738 des Stickstoffs in organischen Körpern. Zeitschrift für analytische Chemie 22, 366–382.
Legendre, P., Legendre, L., 2012. Numerical Ecology. Elsevier, Amsterdam.
Lenth, R.V., 2016. Least-squares means: The R package lsmeans. Journal of Statistical Software 69, 1–33.
Lucas-Borja, M.E., Hedo, J., Cerdá, A., Candel-Pérez, D., Viñegla, B., 2016. Unravelling the importance of forest age stand and forest structure driving microbiological soil properties, enzymatic activities and soil nutrients content in Mediterranean Spanish black pine (*Pinus nigra* Ar. ssp. *salzmannii*). Forest. Science of The Total Environment 562, 145–154.
Maes, SL, Perring, MP, Vanhellemont, M, Depauw, L., Van den Bulcke, J., Brümelis, G., Brunet, J., Decocq, G., den Ouden, J., Härdtle, W., Hédl, R., Heinken, T., Heinrichs, S., Jaroszewicz, B., Kopecký, M., Máliš, F., Wulf, M., Verheyen, K., 2019. Environmental drivers interactively affect individual tree growth across temperate European forests. Global Change Biology 25, 201–217.
M.A.P.A., 1986. Metodos oficiales de analisis. Tomo III. Mundi-Prensa, Madrid.
MAGRAMA, 2007. In: Ministerio de Agricultura, A.y.M.A. (Ed.), Tercer Inventario Forestal Nacional (IFN3). Ministerio de Agricultura, Alimentación y Medio Ambiente, Spain.
Martínez-Vilalta, J., Lloret, F., Breshears, D., 2011. Drought-induced forest decline: causes, scope and implications. Biology Letters 689–691.
Mausolf, K., Härdtle, W., Jansen, K., Delory, B.M., Hertel, D., Leuschner, C., Temperton, V.M., von Oheimb, G., Fichtner, A., 2018. Legacy effects of land-use modulate tree growth responses to climate extremes. Oecologia 187, 825–837.
McArdle, B.H., Anderson, M.J., 2001. Fitting multivariate models to community data: A comment on distance-based redundancy analysis. Ecology 82, 290–297.
McKenzie, N.J., Jacquier, D.J., Isbell, R.F., Brown, K.L., 2004. Australian Soils and Landscapes An Illustrated Compendium. CSIRO Publishing, Collingwood, Victoria.

Nakagawa, S., Johnson, P.C.D., Schielzeth, H., 2017. The coefficient of determination R^2 and intra-class correlation coefficient from generalized linear mixed-effects models revisited and expanded. Journal of the Royal Society Interface 14, 20170213.

Natalini, F., Alejano, R., Vázquez-Piqué, J., Cañellas, I., Gea-Izquierdo, G., 2016. The role of climate change in the widespread mortality of holm oak in open woodlands of Southwestern Spain. Dendrochronologia 38, 51–60.

Olea, L., San Miguel, A., 2006. The Spanish dehesa: a traditional Mediterranean silvopastoral system linking production and nature conservation. In: 21st General Meeting of the European Grassland Federation, April 3–6, 2006. Badajoz (Spain).

Oksanen, J., Blanchet, F.G., Friendly, M., Kindt, R., Legendre, P., McGlinn, D., Minchin, P.R., O'Hara, R.B., Simpson, G.L., Solymos, P., Stevens, M.H.M., Szoecs, E., Wagner, H., 2013. vegan: Community Ecology Package. R package version 2.0-7. http://CRAN.R-project.org/package=vegan.

Pasho, E., Camarero, J.J., de Luis, M., Vicente-Serrano, S.M, 2011. Impacts of drought at different time scales on forest growth across a wide climatic gradient in north-eastern Spain. Agricultural and Forest Meteorology 151, 1800–1811.

Piccolo, M.C., Neill, C., Cerri, C.C., 1994. Net nitrogen mineralization and net nitrification along a tropical forest-to-pasture chronosequence. Plant and Soil 162, 61–70.

Pinheiro, J.C., Bates, D.M., DebRoy, S., Sarkar, D., R Core Team, 2020. Nlme: linear and nonlinear mixed effects models. R package version 3, 1–147. URL. https://CRAN.R-project.org/package=nlme.

Pulido, F., Díaz, M., Hidalgo de Trucios, S.J., 2001. Size structure and regeneration of Spanish holm oak *Quercus ilex* forests and dehesas: effects of agroforestry use on their long-term sustainability. Forest Ecology and Management 146, 1–13.

R Core Team, 2020. R (v. 4.0.0, 2020): A Language and Environment for Statistical Computing. R Foundation for Statistical Computing, Vienna, Austria. URL. http://www.Rproject.org/.

Rinn, F., 2004. LINTAB 5: Tree-Ring Measurement Station (Electronic Brochure). RINNTECH, Germany, Heidelberg.

Rodá, F., Retana, J., Gracia, C.A., Bellot, J., 1999. Ecology of Mediterranean Evergreen Oak Forests. Springer-Verlag, Berlin, Heidelberg, Germany.

Rolo, V., Moreno, G., 2019. Shrub encroachment and climate change increase the exposure to drought of Mediterranean wood-pastures. Science of the Total Environment 660, 550–558.

Sala, A., Woodruff, D.R., Meinzer, F.C., 2012. Carbon dynamics in trees: feast or famine? Tree Physiology 32, 764–775.

Sangüesa-Barreda, G., Camarero, J.J., Oliva, J., Montes, F., Gazol, A., 2015. Past logging, drought and pathogens interact and contribute to forest dieback. Agricultural and Forest Meteorology 208, 85–94.

Sevilla, C., Villalón, M., Sánchez, J., 2016. Geoportal SIGNA v.3.0 del IGN-CNIG Funcionalidades y novedades. Mapping 4, 40–47.

Stovall, A.E.L., Shugart, H., Yang, X., 2019. Tree height explains mortality risk during an intense drought. Nature Communications 10, 4385.

Stokes, M., Smiley, T., 1968. An introduction to tree-ring dating. University of Chicago Press, Chicago, Illinois, USA.

Schweingruber, F.H., 1990. Anatomy of European Woods. Swiss Federal Research Institute WSL. Birmensdorf, Paul Haupt, Berne, Stuttgart, Vienna.

Vicente-Serrano, S.M., Beguería, S., López-Moreno, J.I., 2010. A multiscalar drought index sensitive to global warming: the standardized precipitation evapotranspiration index. Journal of Climate 23, 1696–1718.

Vicente-Serrano, S.M., Tomas-Burguera, M., Beguería, S., Reig, F., Latorre, B, Peña-Gallardo, M., Luna, M.Y., Morata, A., González-Hidalgo, J.C., 2017. A high resolution dataset of drought indices for Spain. Data 2, 22.